Temperature Response of Self-Assembled Micelles of Telechelic Hydrophobically Modified Poly(2-alkyl-2-oxazoline)s in Water

Rodolphe Obeid,[†] Elena Maltseva,[‡] Andreas F. Thünemann,[‡] Fumihiko Tanaka,[§] and Françoise M. Winnik*,[†]

Department of Chemistry and Faculty of Pharmacy, University of Montreal, CP 6128 Succursale Centre Ville, Montreal, QC H3C 3J7, Canada; BAM Federal Institute for Materials Research and Testing, Richard Willstätter Strasse 11, 12489 Berlin, Germany; and Department of Polymer Science, Kyoto University, Katsura, Nishikyo-ku, Kyoto 615-8510, Japan

Received November 18, 2008; Revised Manuscript Received January 15, 2009

ABSTRACT: Hydrophobically end-modified (HM) poly(2-ethyl-2-oxazolines) (PEtOx) and poly(2-isopropyl-2-oxazolines) (PiPrOx) bearing an *n*-octadecyl chain on both termini or on one chain end only were prepared by cationic ring-opening polymerization of 2-ethyl-2-oxazoline and 2-isopropyl-2-oxazoline, respectively, and subsequent end-group modification. The polymers had a molar mass (M_n) ranging from 7000 to 13 000 g mol^{-1}, a size distribution $M_w/M_n < 1.20$, and end-group functionality > 0.97. All polymers, except the semitelechelic sample C_{18}-PiPrOx-OH 13K (M_n = 13 000 g mol^{-1}), formed core−shell micelles in cold water with a hydrodynamic radius (R_H), measured by dynamic light scattering, between 7 and 12 nm and a core of radius (R_c), determined by analysis of small-angle X-ray scattering (SAXS) data, of ∼1.3 nm. Aqueous solutions of all polymers underwent a heat-induced phase transition detected by an increase in solution turbidity at a temperature (T_{cp}, cloud point) ranging from 32 to 62 °C, depending on polymer structure and size. Temperature-dependent light scattering (LS) measurements and fluorescence depolarization studies with the probe diphenylhexatriene (DPH) revealed that extensive intermicellar bridging takes place in solutions heated in the vicinity of T_{cp} leading to large assemblies ($R_H \geq 1$ μm). Further heating caused these assemblies to shrink into objects with $R_H \sim 300-700$ nm, depending on the size and structure of the polymer. The formation of H-bonds between water molecules and the main-chain amide nitrogen atoms imparts distinct features to the flower/star micelles formed by telechelic/semitelechelic PiPrOx and PEtOx, compared to the micelles formed by other hydrophobically end-modified water-soluble polymers, such as poly(ethylene oxide) or poly(*N*-isopropylacrylamide).

Introduction

The creation of organized nanostructured materials and fluids remains one of the major challenges in polymer science, even though it has been the focus of intensive research over several decades. The current thrust in this field is geared toward the design of waterborne organized systems, partly for environmental considerations and partly in view of specific needs in biotechnology and medicine. Amphiphilic polymers consisting of a water-soluble block linked to two hydrophobic chains, also known as associative polymers, have proven to be particularly useful in this context. The structure of associative polymers can be tailored at will so that their aqueous solutions exhibit rheological properties enabling applications in coatings, oil production and transportation fluids, water treatment systems, or as thickeners for food and health care products.[1] In most cases, the hydrophilic moiety is poly(ethylene oxide) (PEO) or a block copolymer with a PEO block and a block of a second hydrophilic monomer. The hydrophobic end groups may be alkyl- or aralkyl chains, as in the case of the industrial polymers known as "hydrophobic ethylene oxide−urethane copolymers" (HEUR),[2] or short water-insoluble blocks made up of poly(ethylene-*co*-propylene) or polystyrene.[3,4] Current research focuses on the design of more complex associative polymers in order to develop stimuli-responsive systems able to respond repeatedly and reversibly to an external trigger, such as a change of solution pH or temperature, or upon irradiation with a beam of light.[5,6] Stimuli-responsive "smart" polymers often contain blocks able to change rapidly from being hydrophobic to hydrophilic, or vice versa, on the basis of acid−base reactions, changes in pH, or irradiation with light of a specific wavelength. They may also take advantage of the changes in the hydration and conformation of a polymer chain in water as the solution is heated or cooled through its lower critical solution temperature (LCST). Poly(*N*-isopropylacrylamide) (PNIPAM) is the most studied thermosensitive water-soluble polymers.[7] Other thermosensitive aqueous polymers of industrial or academic interest include cellulose ethers,[8] certain poly(2-alkyl-2-oxazolines),[9] and poly(methyl vinyl ether)[10] as well as various poly(acrylates) and poly(methacrylates).[11]

We reported recently the synthesis and properties of a family of thermoresponsive associative polymers consisting of a PNIPAM chain carrying an *n*-octadecyl group at each chain end (C_{18}-PNIPAM-C_{18}).[12,13] In aqueous media below their LCST, the C_{18}-PNIPAM-C_{18} samples self-assemble following the well-established patterns typical of HEUR copolymers: formation of flower micelles in solutions of low concentration and, above a critical concentration, intermicellar bridging leading to clusters of micelles and, eventually, to a cross-linked micellar network. Aqueous C_{18}-PNIPAM-C_{18} solutions also respond to changes in temperature in a controlled manner: in the dilute regime, they form stable mesoglobules in solutions heated above the LCST,[14] while in the concentrated regime, syneresis takes place. We describe here a new class of thermoresponsive associative polymers in which the water-soluble main chain is either poly(2-ethyl-2-oxazoline) (PEtOx) or poly(2-isopropyl-2-oxazoline) (PiPrOx). Poly(2-alkyl-2-oxazolines), where the alkyl group is methyl, ethyl, or isopropyl, are biocompatible, biodegradable, and possess stealth characteristics in vitro and in vivo comparable to those of poly(ethylene glycols).[15] They are used increasingly as biomaterials, hydrogels, proteins

* Corresponding author: Ph (514) 340 5179; Fax (514) 340 5292; e-mail francoise.winnik@umontreal.ca.
[†] University of Montreal.
[‡] BAM Federal Institute for Materials Research and Testing.
[§] Kyoto University.

10.1021/ma802592f CCC: $40.75
Published on Web 02/18/2009

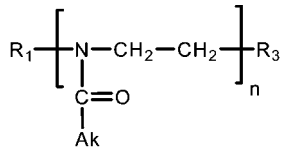

C_{18}-PAkOx-C_{18}: $R_1 = R_2 = C_{18}H_{37}$-, Ak = -CH_2-CH_3, -$CH(CH_3)_2$
C_{18}-PAkOx-OH: $R_1 = C_{18}H_{37}$-, Ak = -CH_2-CH_3, -$CH(CH_3)_2$, R_2 = OH
Me-PiPrOx-OH: R_1 = -CH_3, Ak = -$CH(CH_3)_2$, R_2 = OH

Figure 1. Structure of the polymers used in this study.

modifiers, antibacterial agents,[16] and drug carriers.[17,18] In water, PEtOx and PiPrOx undergo a phase transition upon heating beyond a specific temperature, the cloud point (T_{cp}), which ranges from approximately 62−100 °C[9,19] and 36−80 °C,[20] respectively, depending on polymer size and concentration. The macroscopic phase separation reflects the dehydration of the polymer chains, followed by aggregation of the denuded nonpolar chains into large particles. In most situations, the phase transition is reversible: cooling the solution below its cloud point triggers the rehydration of the polymer chains, and the solution recovers its limpidity. It has been reported recently that if aqueous solutions of PiPrOx are kept well above their cloud point (e.g., 65 °C) for extended periods of time (24 h), the phase-separated PiPrOx chains crystallize into water-insoluble fibrils.[21,22] In contrast, PEtOx is an amorphous polymer[23] and shows no tendency to crystallize from hot water. There have been only a few reports so far on the preparation of telechelic or semitelechelic hydrophobically modified poly(oxazolines). Volet et al.[24] have described the synthesis and solution properties of semitelechelic poly(2-methyl-2-oxazolines) bearing an *n*-dodecyl- or an *n*-octadecyl group at one chain end. Telechelic poly(2-methyl-2-oxazolines) with a perfluorooctyl group at one end and a hydrocarbon group 6−18 carbons long were prepared with a view toward the creation of multidomain micelles containing segregated fluorinated and hydrocarbon hydrophobic compartments.[25]

We report here the synthesis of a series of α,ω-di-*n*-octadecyl poly(2-isopropyl-2-oxazolines) (C_{18}-PiPrOx-C_{18}) of various molecular weights, together with their semitelechelic homologues, α-*n*-octadecyl-ω-hydroxy-poly(2-isopropyl-2-oxazolines) (C_{18}-PiPrOx-OH) and a pair of telechelic/semitelechelic poly(2-ethyl-2-oxazolines) (C_{18}-PEtOx-C_{18} and C_{18}-PEtOx-OH) (Figure 1). We employed dynamic and static light scattering (DLS and SLS) to gain information on the size and aggregation number of the polymeric micelles formed in cold aqueous solutions and to monitor their fate as a function of temperature. Using small-angle X-ray scattering (SAXS) measurements, we determined the size of the micellar core and evaluated the micelle aggregation number. Static fluorescence measurements were carried out with poly(oxazoline) aqueous solutions containing small amounts of pyrene (Py) to determine the onset of micellization and the micelle aggregation number. Fluorescence depolarization studies were conducted using diphenylhexatriene to assess the microviscosity of the hydrophobic core of hydrated micelles and of the aggregates formed above the solutions LCST. The results are discussed in the context of the current understanding of the association of telechelic amphiphilic copolymers, based on previous reports on the solution properties of telechelic hydrophobically modified poly(ethylene oxides) and poly(*N*-isopropylacrylamides).

Experimental Section

Materials. All chemicals were purchased from Sigma-Aldrich Chemicals Co. and used as received, unless otherwise stated. 2-Isopropyl-2-oxazoline was prepared from isobutyric acid and 2-aminoethanol following a known procedure[26] and purified by two consecutive vacuum distillations over calcium hydride (CaH_2). It was used to prepare derivatized poly(2-isopropyl-2-oxazolines) (see below) and a sample of α-hydroxy-ω-methyl poly(2-isopropyl-2-oxazoline) (Me-PiPrOx-OH 10K) (M_n = 10 400 g mol^{-1}, PDI = 1.06) obtained by cationic ring-opening polymerization initiated with methyl *p*-tosylate, following a known procedure.[20] Acetonitrile (Accusolv) and chloroform were dried by reflux over CaH_2 under a dry nitrogen atmosphere and subsequently distilled prior to use. Methanolic KOH was prepared by addition of potassium hydroxide (KOH) pellets into methanol. Water was deionized with a Millipore Milli-Q system.

Preparation of α-*n*-Octadecyl-ω-hydroxypoly(2-alkyl-2-oxazolines) (C_{18}-PAkOx-OH). The polymers were prepared by cationic ring-opening polymerization of either 2-ethyl-2-oxazoline or 2-isopropyl-2-oxazoline initiated with *n*-octadecyl-4-chlorobenzenesulfonate. The procedure, exemplified here in the case of C_{18}-PiPrOx-OH 7K, was followed to prepare all polymers using the monomer/initiator ratios and reaction times listed in Table 1. 2-Isopropyl-2-oxazoline (5 mL, 49.55 mmol) was added with a syringe to a solution of *n*-octadecyl-4-chlorobenzenesulfonate (220 mg, 0.5 mmol) in acetonitrile (20 mL) kept under dry nitrogen. The polymerization mixture was heated at reflux (80 °C) for 48 h. The mixture was cooled to room temperature and treated with methanolic KOH (0.1 N) to introduce a hydroxyl group at one chain end. The polymer was isolated by precipitation into diethyl ether. It was dissolved in water and purified by dialysis against distilled water for 3 days using a Spectra/Por CE membrane (MWCO: 6000−8000 g mol^{-1}) and isolated by freeze-drying; yield: 3.46 g; 71%. ^{1}H NMR ($CDCl_3$) ppm, δ: 0.9 (t, C*H*$_3$−(CH$_2$)$_{17}$−), 1.11 (br s, CO−CH−(C*H*$_3$)$_2$), 1.27 (s, CH$_3$−(C*H*$_2$)$_{17}$−N−), 2.7−2.9 (br m, CO−C*H*−(CH$_3$)$_2$), 3.48 (br m, −N−*CH*$_2$-*CH*$_2$−).

Preparation of α,ω-Di-*n*-octadecyl-(2-alkyl-2-oxazolines) (C_{18}-PAkOx-C_{18}). The synthesis is exemplified in the case of C_{18}-PiPrOx-C_{18} 7K. The same procedure was followed to prepare all polymers, starting with the appropriate semitelechelic polymer. A solution of C_{18}-PiPrOx-OH 7K (2.0 g, 17.7 mmol OH) in dry $CHCl_3$ (13.5 mL, freshly distilled from CaH_2) was heated to 60 °C for 5 min under nitrogen to ensure complete dissolution of the polymer. *n*-Octadecyl isocyanate (0.088 g, 0.298 mmol) was added to the solution, followed by dibutyltin laurate (10 drops). The reaction mixture was kept at 60 °C under dry nitrogen. After 12 h, *n*-octadecyl isocyanate (0.264 g, 0.894 mmol) was added to the reaction mixture to ensure quantitative end-capping. The reaction mixture was kept at 60 °C for another 24 h. It was cooled to room temperature. The polymer was isolated by precipitation into hexanes. It was redissolved into $CHCl_3$. The solution was filtered through a 0.45 μm filter. The polymer was precipitated into hexanes and dried in vacuum; (1.8 g, 90%). ^{1}H NMR ($CDCl_3$) ppm, δ: 0.9 (t, C*H*$_3$−(CH$_2$)$_{17}$−), 1.11 (br s, CO−CH−(C*H*$_3$)$_2$), 1.27 (s, CH$_3$−(C*H*$_2$)$_{17}$−N−), 2.7−2.9 (br m, −CO−C*H*−(CH$_3$)$_2$), 3.48 (br m, −N−*CH*$_2$−*CH*$_2$−). The efficiency of the conversion (C_{eff}) of semitelechelic polymers into telechelic polymers was determined from the relationship

$$C_{eff} = 2 \times \frac{(n_{CH_2}/n_{CH_3})_{NMR}}{(n'_{CH_2}/n'_{CH_3})_{GPC}} \quad (1)$$

where n_{CH_2} and n'_{CH_2} are the numbers of methylene protons of the *n*-octadecyl chains obtained from ^{1}H NMR and GPC data, respectively, and n_{CH_3} and n'_{CH_3} are the numbers of methyl protons of the isopropyl or ethyl moieties of the repeat unit, obtained from ^{1}H NMR and GPC data, respectively. All α,ω-di-*n*-octadecyl-(2-ethyl-2-oxazolines) readily dissolved in water. However, α,ω-di-*n*-octadecyl-(2-isopropyl-2-oxazolines) recovered after precipitation were only soluble in water up to a concentration of ∼ 2.0 g L^{-1}. In order to enhance the solubility in water, polymers were dissolved in dimethyl sulfoxide (DMSO) and dialyzed against water for 3 days using membranes of MWCO 1000 g mol^{-1}. The polymers

Table 1. Polymerization Conditions and Properties of the Polymers Investigated

polymer	reaction time (h) at 80 °C	[AkOx]/[I][a]	M_n[c]	M_w/M_n[c]	n[d]	hydrophobe per chain[e]	T_{cp}[f]/°C
Me-PiPrOx-OH 10K	72	100[b]	10 400	1.06	90		44
C_{18}-PEtOx-OH 10K	72	100	9 700	1.12	95	0.99	62.4
C_{18}-PiPrOx-OH 7K	40	60	6 700	1.21	57	0.99	32.5
C_{18}-PiPrOx-OH 10K	72	100	9 900	1.17	85	0.98	33.2
C_{18}-PiPrOx-OH 13K	120	140	12 800	1.16	111	0.99	39
C_{18}-PEtOx-C_{18} 10K	48		10 100	1.11	95	2.00	57.1
C_{18}-PiPrOx-C_{18} 7K	48		7 000	1.15	57	1.98	31.6
C_{18}-PiPrOx-C_{18} 10K	48		10 300	1.15	85	1.99	32.1
C_{18}-PiPrOx-C_{18} 13K	48		13 100	1.18	111	1.97	34.9

[a] I: initiator (*n*-octadecyl-4-chlorobenzenesulfonate). [b] I: methyl *p*-tosylate. [c] M_n and M_w: number- and weight-average molecular weight from GPC analysis. [d] Number of monomer units. [e] From ^{1}H NMR. [f] T_{cp}: cloud point, from turbidity measurements (polymer concentration: 1.0 g L^{-1}).

recovered by lyophilization of the dialysates dissolved readily in water up to a concentration of 20 g L^{-1}.

Instrumentation. All ^{1}H NMR spectra were recorded on a Bruker AMX-400 (400 MHz) spectrometer. Variable temperature ^{1}H NMR spectra were recorded using polymer solutions (2.0 g L^{-1}) in D_2O (D, 99.9%). For each temperature, the solution was equilibrated for 20 min before acquiring the data. Fourier transform infrared (FTIR) spectra were recorded on a Perkin-Elmer spectrometer using dispersions of polymer powders in potassium bromide (KBr) pellets. A total of 256 scans were signal-averaged in the range from 4000 to 400 cm^{-1} at a resolution of 4 cm^{-1}. UV−vis spectra were recorded on an Agilent 8452A photodiode array spectrometer used also for turbidity measurements. Gel permeation chromatography (GPC) was performed on a GPC-MALLS system consisting of an Agilent 1100 isocratic pump, a set of TSK-gel α-M (particle size 13 μm, exclusion limit 1×10^7 g mol^{-1} for polystyrene in DMF) and a TSK-gel α-3000 (particle size 7 μm, exclusion limit 1×10^5 g mol^{-1} for polystyrene in DMF) (Tosoh Biosep) columns, a Dawn EOS multiangle laser light scattering detector $\lambda = 690$ nm (Wyatt Technology Co.), and an Optilab DSP interferometric refractometer $\lambda = 690$ nm (Wyatt Technology Co.) under the following conditions: injection volume, 100 μL; flow rate, 0.5 mL min^{-1}; eluent, DMF; temperature, 40 °C, using d*n*/d*c* values of the derivatized PEtOx (0.074 mL g^{-1}) and the derivatized PiPrOx (0.084 mL g^{-1}) in DMF (λ; 690 nm, 40 °C).

Fluorescence Measurements. Steady-state fluorescence spectra were recorded on a Varian Cary Eclipse spectrometer equipped with a GRAMS/32 data analysis system. For fluorescence depolarization measurements, the spectrometer was fitted with two Glan-Thompson polarizers in the L-format configuration. Temperature control of the samples was achieved using a water-jacketed cell holder connected to a Cary circulating water bath. The temperature of the sample fluid was measured with a thermocouple immersed in a water-filled cell placed in one of the four cell holders in the sample compartment. All measurements were carried out at 24 °C, unless stated otherwise.

Determination of c_{mic} and N_{agg}. Slit widths were set at 5 and 2.5 nm for the excitation and emission monochromators, respectively. Pyrene fluorescence spectra were recorded from 360 to 600 nm using an excitation wavelength of 334 nm. To determine the onset of micellization (c_{mic}) solutions of polymer concentration ranging from 3.0 to 10^{-4} g L^{-1} were prepared by dilution of a polymer stock solution (3.0 g L^{-1}) in water containing pyrene (Py $\sim 10^{-6}$ M). The aqueous pyrene solution was prepared as follows: A solution of pyrene in ethanol (10 μL, 6.5×10^{-3} M) was added to an empty flask. The ethanol was evaporated with a stream of argon to form a thin film on the bottom of the flask, followed by addition of water. Solutions were stirred at room temperature for 48 h prior to measurement. The emission intensities measured at 373 nm (I_1) and 383 nm (I_3), the first and third vibronic peaks in the fluorescence emission spectrum of pyrene, were used to calculate the ratio I_1/I_3. To determine the aggregation number of the polymer micelles, polymer solutions of various concentrations (2.0−6.0 g L^{-1}) were prepared in water containing $\sim 10^{-6}$ M Py. The solutions were stirred at room temperature for 48 h. Aliquots (10 μL) of an aqueous solution of cetylpyridinium chloride (CPC) (1.5×10^{-4} M) were added to the polymer/Py solution immediately prior to fluorescence measurements. Control DLS measurements confirmed that the addition of CPC to the polymer solution does not affect significantly the size of the micelles. The aggregation number (N_{agg}) was estimated[27] using eq 2, where I/I_0 is the ratio of Py fluorescence intensities at 383 nm in the presence and in the absence of the quencher (Q), respectively, [Q] is the quencher concentration, [C_{18}] is the concentration of *n*-octadecyl groups, and [M] is the concentration of micelles. A plot of ln I_0/I against [Q] gives a straight line, the slope of which corresponds to [M]$^{-1}$.

$$\ln \frac{I_0}{I} = \frac{[Q]}{[M]} \quad \text{with } N_{agg} = \frac{[C_{18}]}{[M]} \tag{2}$$

Anisotropy Measurements. The slit settings were 2.5 nm for both excitation and emission monochromators. The probe was 1,6-diphenyl-1,3,5-hexatriene (DPH). The excitation and emission wavelengths were set at 360 and 428 nm, respectively. The fluorescence anisotropy (r) was calculated from the relationship

$$r = \frac{I_{VV} - GI_{VH}}{I_{VV} + 2GI_{VH}} \tag{3}$$

where $G = I_{VH}/I_{HH}$ is an instrumental correction factor and I_{VV}, I_{VH}, and I_{HH} refer to the resultant emission intensities at 428 nm polarized in the vertical or horizontal planes (second subindex) upon excitation with either vertically or horizontally polarized light (first subindex). The values reported in the text are averages of five measurements (standard error ±0.01). Samples for analysis were prepared as follows. A stock solution of DPH (10 μL, 0.5 mM) in tetrahydrofuran was placed in a flask. The solvent was removed under a stream of nitrogen. Water was added in the flask such that the final DPH concentration was 1.0 μM. Polymer/DPH solutions (1.0 g L^{-1}) were prepared by dissolving each polymer in aqueous DPH (1.0 μM). The mixture was stirred vigorously at room temperature overnight. Fluorescence depolarization data were recorded at fixed temperature intervals while polymer/DPH solutions were heated at a constant rate (~2 °C min^{-1}) from 17 to 53 °C within the spectrometer sample holder.

Turbidity Measurements. Cloud points were determined by spectrometric detection of the changes in turbidity ($\lambda = 550$ nm) of aqueous polymer solutions (1.0 g L^{-1}) heated at a constant rate (1 °C min^{-1}). The cloud point value reported is the temperature corresponding to a decrease of 20% of the solution transmittance. The estimated error in T_{cp} determined by this procedure is ±0.5 °C.

Light Scattering Measurements. Static (SLS) and dynamic (DLS) light scattering experiments were performed on a CGS-3 goniometer (ALV GmbH) equipped with a ALV/LSE-5003 multiple-τ digital correlator (ALV GmbH), a He−Ne laser ($\lambda = 633$ nm), and a C25P circulating water bath (Thermo Haake). SLS experiments yield the apparent weight-average molar mass ($M_{w,app}$) and the z-average root-mean square radius of gyration (R_G) of scattering objects in dilute solution, based on the angular dependence of the excess absolute scattering intensity, known as the excess Rayleigh ratio $R(q,c)$ given by eq 4:

$$\frac{K(c-c_{mic})}{R(q,c)} \cong \frac{1}{M_{w,app}P(\Theta)} + 2A_2(c-c_{mic}) \quad (4)$$

where c is the polymer concentration, c_{mic} is the concentration of micellization onset, q is the scattering vector ($q = (4\pi n/\lambda)\sin(\Theta/2)$), A_2 is the second virial coefficient, n is the refractive index of the solvent, λ is the wavelength of the light in the vacuum, and Θ is the scattering angle (30°−150°). The scattering constant is $K = 4\pi^2 n^2 (dn/dc)^2/N_A\lambda^4$, where dn/dc is the refractive index increment and N_A is Avogadro's number. The dn/dc of the derivatized PEtOx and the derivatized PiPrOx were 0.172 and 0.213 mL g^{-1}, respectively, for aqueous solutions at 24 °C and a wavelength of 690 nm. In eq 4, it is assumed that the contribution of a single polymer chain to the scattering intensity is negligible, compared to that of the micelles. Data recorded for solutions of concentration c were analyzed according to the Zimm equation, assuming that the macromolecules are in a swollen conformation. In this case, the particle scattering function is $P(\Theta) = 1 - (q^2R_G^2)/3$, where R_G is the radius of gyration. Since $(q^2R_G^2)/3 \ll 1$, it may be assumed that $1/[1 - (q^2R_G^2)/3] \cong 1 + (q^2R_G^2)/3$. Thus, eq 4 becomes

$$\frac{K(c-c_{mic})}{R(q,c)} \cong \frac{1}{M_{w,app}}\left(1 + \frac{R_G^2}{3}q^2\right) + 2A_2(c-c_{mic}) \quad (5)$$

The apparent mass of a polymer ($M_{w,app}$) in a solution of concentration c was obtained by extrapolation of the scattered intensity $R(q,c)/(c - c_{mic})$ to $q = 0$. The apparent radius of gyration of of the scattering objects in a solution of concentration c was obtained by a mean-square linear fit of the inverse of the scattered intensity versus q^2 (see eq 5). See Supporting Information for details of the analysis and examples of plots of the inverse of the scattering intensity vs q^2 (Figure S1.1). The traditional Zimm plot analysis could not be carried out with these samples as a result of the coexistence, depending on the solution concentration, of micelles and unimers or of micelles and larger aggregates. Similar observations were reported in previous studies of telechelic and semitelechelic poly(ethylene oxides)[28−30] and telechelic PNIPAM.[14]

In DLS experiments, one measures the normalized time autocorrelation function of the scattered intensity, which can be expressed in terms of the autocorrelation function of the concentration fluctuations. In our experiments, the relaxations had always a diffusive character with a characteristic time (τ) inversely proportional to q^2. A cumulant analysis was applied to obtain the diffusion coefficient (D) of the scattering objects in solution. Extrapolation of the first reduced cumulant $(\tau q^2)^{-1}$ to $q = 0$ yields the value of D, which is related to the average hydrodynamic radius R_H of the scattering objects by eq 6:

$$D = \frac{k_B T}{6\pi\eta_S R_H} \quad (6)$$

where η_S the viscosity of the solvent, k_B is the Boltzmann constant, and T is the absolute temperature. In some cases, the average relaxation time was determined by the CONTIN analysis based on the inverse Laplace transform of the normalized dynamical correlation function of the polymer concentration fluctuations. This method is more appropriate for solutions characterized by several relaxation mechanisms. It was found that the relaxation times obtained using this method coincides, within experimental uncertainties, with those calculated by the cumulant analysis.

Solutions for DLS and SLS analysis were prepared by two different methods: (i) a polymer stock solution (20.0 g L^{-1}) in water was obtained by direct dissolution of the polymer and gentle stirring at room temperature for at least 12 h. The stock solution was used to prepare solutions ranging in concentration from 0.5 to 20.0 g L^{-1}; (ii) the polymer was first dissolved in ethyl alcohol. Deionized water was added dropwise to a solution of the polymer in ethanol. The ethanol was eliminated by dialysis against water during 3 days using Spectra-Por membranes (MWCO 6000−8000 g mol^{-1}). Identical LS data were obtained for solutions of a given polymer, independently of the preparation method. Solutions were kept at room temperature for at least 12 h prior to analysis. They were filtered through a 0.45 μm Millex Millipore PVDF filter directly into the sample cell. In some experiments with solutions of telechelic PiPrOx, samples were subjected to ultrasonication for 15 min using a W450 digital sonifier (Branson). Sonicated solutions were stored for 24 h at room temperature. For temperature-dependent measurements, polymer solutions (1.0 g L^{-1}) were placed in the system sample holder and equilibrated at a set temperature for 30 min prior to measurement. Three measurements of 1 min each were carried out and averaged, and then the sample was brought to a higher temperature and subjected to the same treatment. A complete experiment (from 20 to 55 °C) took ∼9 h.

To determine the size of particles of $R_H > \sim 1$ μm, for which multiple scattering effects are significant, we used a Zetasizer Nano ZS light scattering apparatus (Malvern Instruments) with a He−Ne laser ($\lambda = 633$ nm). The Nano ZS instrument incorporates noninvasive backscatter (NIBS) optics with a detection angle of 173°. In this configuration, which allows one to change measurement position within the cell, the illuminating beam and the detected light do not need to travel through the entire sample, reducing the extent of multiple scattering. The size of particles was determined by cumulant analysis using the software supplied by the manufacturer.

Small-Angle X-ray Scattering (SAXS) Measurements. SAXS measurements were performed on a SAXSess instrument (Anton Paar, Austria) attached to a laboratory X-ray generator (PW3830, PANalytical) equipped with a fine focus glass PW1316/92 X-ray tube and operated at 40 kV and 50 mA. The monochromatic primary beam (Cu Kα, $\lambda = 0.154$ nm) was attenuated by a Ni semitransparent beam stop that enables normalization of the scattered intensity to the primary intensity (intensity at $q = 0$). The scattered intensities were recorded with a cooled (−40 °C) CCD camera (PI-SCX, Princeton Instruments) in the line collimation geometry and integrated into the one-dimensional scattering function $I(q)$ using the SAXSQuant 1D software (Anton-Paar, Austria). Solutions for analysis were prepared as follows: the polymer was first dissolved in ethyl alcohol. Deionized water was added dropwise to a solution of the polymer in ethanol. The ethanol was eliminated by dialysis against water for 3 days using Spectra-Por membranes (MWCO 6000−8000 g mol^{-1}). Solutions for analysis were poured at room temperature in vacuum-tight thin quartz capillaries and placed in a TCS 120 temperature-controlled sample holder. Background contributions from capillary and solvent scattering were subtracted from the sample scattering. The scattering vector q, defined as $q = 4\pi/\lambda \sin\theta$, where θ is the scattering angle and λ the wavelength of the radiation, varied in the 0.2−3.0 nm^{-1} range. In all our calculations for core/shell micelles we have used the program Scatter Version 2.0 created by Stefan Förster (University of Hamburg) which is based on general expressions and scattering functions derived in his previous work.[31]

Results and Discussion

Polymer Synthesis and Characterization. The hydrophobically modified telechelic poly(2-alkyl-2-oxazolines) (C_{18}-PEtOx-C_{18} and C_{18}-PiPrOx-C_{18}) were prepared in two steps by a sequence, depicted in Figure 2, which generates pairs of telechelic and semitelechelic polymers of identical molecular weight but different end groups. The semitelechelic PAkOx samples were obtained by cationic ring-opening polymerization of the corresponding 2-alkyl-2-oxazoline initiated with *n*-octadecyl-4-chorobenzenesulfonate and quenched with methanolic KOH, a procedure that introduces an *n*-octadecyl group at the α end and a hydroxyl group at the ω chain end. The molecular weight of the polymers was adjusted by varying the reaction time and the initiator/monomer molar ratio (Table 1). The purified hydroxyl-terminated polymers were reacted with *n*-octadecylisocyanate under conditions developed for the synthesis of amphiphilic telechelic poly(ethylene oxides),[2,32,33] yielding the desired α,ω-di-*n*-octadecyl-poly(2-alkyl-2-oxazolines). The

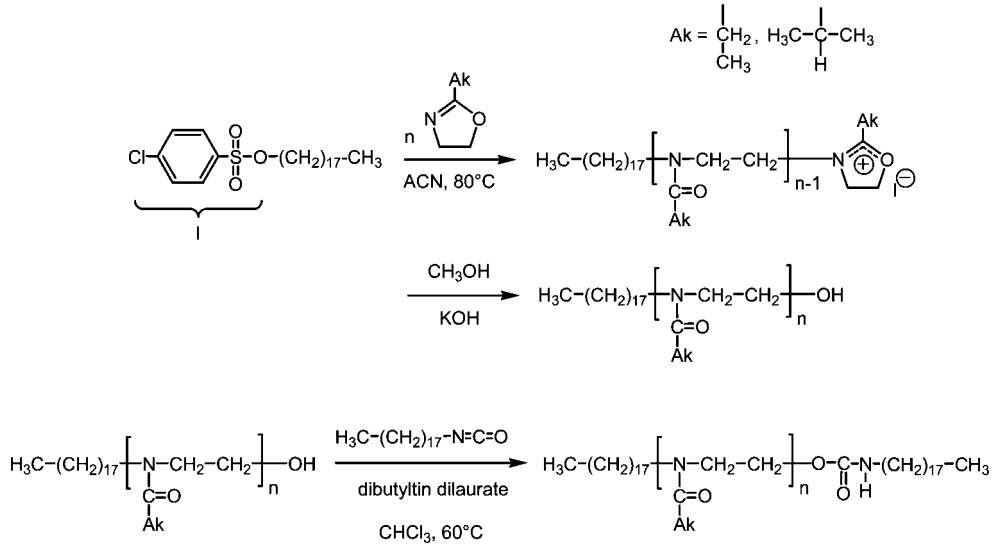

Figure 2. Reaction schemes for the cationic ring-opening polymerization of 2-alkyl-2-oxazolines initiated by *n*-octadecyl-4-chlorobenzenesulfonate (C_{18}-PAkOx-OH) and the preparation of PAkOx derivatives (C_{18}-PAkOx-C_{18}).

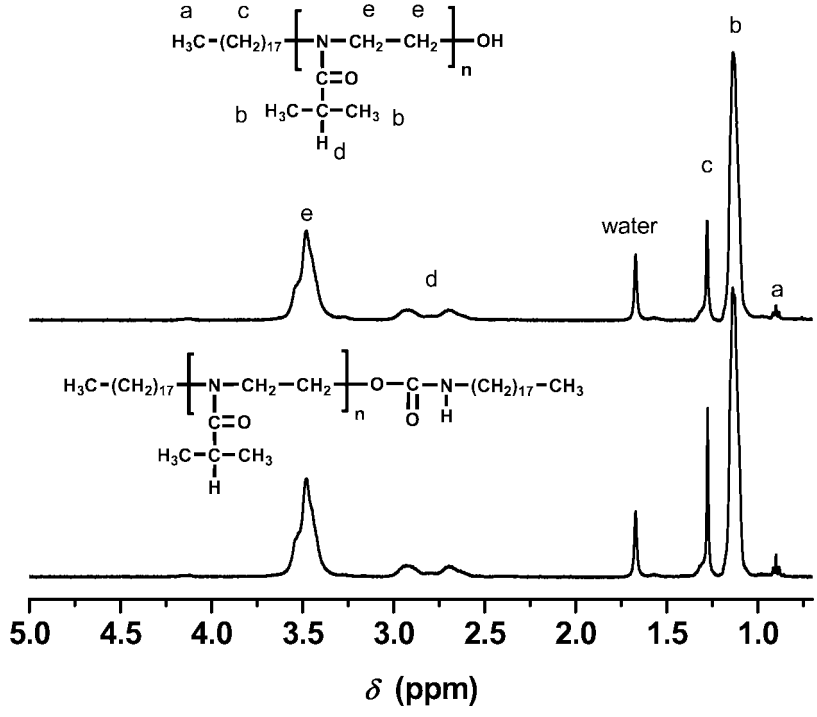

Figure 3. ^{1}H NMR spectra of C_{18}-PiPrOx-OH 7K (top) and C_{18}-PiPrOx-C_{18} 7K (bottom); solvent: $CDCl_3$.

efficiency of the conversion of semitelechelic polymers into telechelic polymers was determined from ^{1}H NMR spectra recorded for polymer solutions in $CDCl_3$, using the signal at $\delta = 1.27$ ppm, attributed to the resonance of the methylene protons of the *n*-octadecyl chains together with the broad singlet at $\delta = 1.11$ ppm (PiPrOx) or $\delta = 1.14$ ppm (PEtOx) ascribed to the resonances of the methyl protons of the isopropyl or ethyl moieties of the repeat units (Figure 3). The polymer functionality exceeded 97% in all cases (Table 1). Further proof of the successful end-capping of the semitelechelic polymers was extracted from the FTIR spectra of the polymers. The FTIR spectrum of the telechelic polymers presents a weak band at ~1730 cm^{-1}, a wavenumber characteristic of the urethane carbonyl group.[34] This band is not observed in the spectrum of the semitelechelic samples, as exemplified in Figure 4 in the case of C_{18}-PiPrOx-OH 7K and C_{18}-PiPrOx-C_{18} 7K. The spectra of both polymers exhibit a strong amide I band (~1656 cm^{-1}) characteristic of the tertiary amide group of the repeat unit, bands around 2977 and 1421 cm^{-1}, characteristic of the stretching and deformation vibration modes of the main-chain methylene groups, a CH_2 scissor band at 1470 cm^{-1}, and the asymmetric and symmetric CH_3 deformation modes at 1458 and 1375 cm^{-1}, respectively.

Self-Assembly of the Modified Poly(2-alkyl-2-oxazolines) (PAkOx) in Water at Room Temperature. On the basis of previous studies of hydrophobically modified poly(ethylene oxides),[35−37] poly(*N*-isopropylacrylamides),[12−14,38] and poly(2-methyl-2-oxazoline),[24,25] bearing one or two hydrophobic end groups, we anticipated that the semitelechelic C_{18}-PAkOx-OH and telechelic C_{18}-PAkOx-C_{18} samples assemble in water in the form of "star micelles" and "flower micelles", respectively. The experiments described below were aimed at confirming the formation of micellar assemblies in aqueous C_{18}-PAkOx-OH

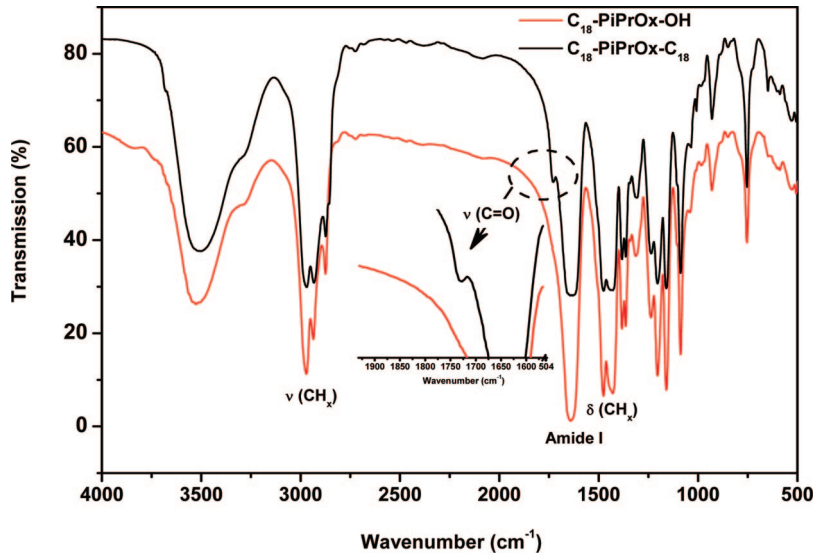

Figure 4. FTIR spectra of C_{18}-PiPrOx-OH 7K (red) and C_{18}-PiPrOx-C_{18} 7K (black).

Table 2. Fluorescence and Light Scattering Data for Solutions of Various HM-PAkOx Samples in Dilute Aqueous Solutions

polymer	c_{mic}[a]/g L^{-1} at $T = 24$ °C	N_{agg} fluor[b]	N_{agg} SLS	$M_{w,app}$ (10^4)	Φ (g/mL)	R_G/nm	R_G/R_H	R_H/nm 24 °C	R_H/nm 50 °C
C_{18}-PEtOx-OH 10K	0.040	21 ± 1	22 ± 2	22 ± 0.2	0.073	13.3 ± 0.3	1.26	10.6 ± 0.3	580 ± 7[d]
C_{18}-PiPrOx-OH 7K	0.012	7 ± 2	8 ± 1	6 ± 0.7	0.060	8.8 ± 0.5	1.22	7.2 ± 0.5	250 ± 7
C_{18}-PiPrOx-OH 10K	0.016	6 ± 1	6 ± 2	6 ± 1.1	0.042	10.4 ± 0.8	1.27	8.2 ± 0.8	260 ± 6
C_{18}-PiPrOx-OH 13K	0.300			1.7 ± 0.1		3.7 ± 0.3	1.28	2.9 ± 0.3	880 ± 20[e]
C_{18}-PEtOx-C_{18} 10K	0.020	13 ± 2	16 ± 1	16 ± 0.1	0.076	11.2 ± 0.5	1.19	9.40 ± 0.5	1000 ± 50[d,e]
C_{18}-PiPrOx-C_{18} 7K	0.006	14 ± 2	13 ± 1	10 ± 0.8	0.086	9.1 ± 0.4	1.20	7.6 ± 0.4	370 ± 8
C_{18}-PiPrOx-C_{18} 10K	0.009	9 ± 1	−[c]					10.5 ± 0.3 126 ± 0.7	630 ± 11
C_{18}-PiPrOx-C_{18} 13K	0.011	6 ± 1	−[c]					7.9 ± 0.5 102 ± 0.4	715 ± 50

[a] From fluorescence probe measurements. [b] From fluorescence quenching experiments. [c] Bimodal size distribution. [d] Values measured at 70 °C. [e] Values measured using a Zetasizer Nano ZS light scattering instrument.

and C_{18}-PAkOx-C_{18} solutions and at characterizing them in terms of size, shape, aggregation number, and (critical) association concentration. Key parameters extracted from this analysis are listed in Table 2. They include the hydrodynamic radius (R_H), the apparent radius of gyration (R_G, for $c = 1.0$ g L^{-1}), the apparent molecular weight ($M_{w,app}$, $c = 1.0$ g L^{-1}), the aggregation number (N_{agg}: number of polymer chains per micelle), and the average polymer density (Φ) of the micelles, defined by eq 7 where N_A is Avogadro's number.

$$\Phi = \left(\frac{M_{w,app}}{N_A}\right)\left(\frac{4}{3}\pi R_H^3\right)^{-1} \quad (7)$$

The R_H value of the semitelechelic polymer of highest molecular weight, C_{18}-PiPrOx-OH 13K, in water (1.0−10.0 g L^{-1}) was ∼2.9 nm, a value expected for isolated chains or clusters of 2−3 chains. Thus, for this polymer the hydrophilic/lipophilic balance is such that micellization does not take place at room temperature throughout the concentration domain probed. The molecular weight of C_{18}-PiPrOx-OH 13K in water ($M_{w,app}$ ∼ 17 000 g mol^{-1}) derived from SLS measurements confirms this conclusion.

The other semitelechelic polymers formed larger assemblies with R_H ranging form 7 to 9 nm, depending on the length and structure of the polymer chain, and unimodal size distributions with a polydispersity index (PDI) of ∼ 0.15 ± 0.02. DLS measurements were performed at different scattering angles (40°−150°). No angular dependence was found for telechelic/semitelechelic samples, the R_H being almost identical at every angle. This suggests that the scattering particles are isotropic objects,[39] such as spheres, as confirmed by the angular dependence of SAXS data presented below. R_H values decreased slightly with increasing solution concentration, the largest shift, from $R_H = 7.2$ nm (1.0 g L^{-1}) to $R_H = 5.2$ nm (20.0 g L^{-1}) being registered in the case of C_{18}-PiPrOx-OH 7K. The R_G/R_H ratio was ∼1.26 for C_{18}-PiPrOx-OH 7K and 10K, which is within the range expected for star polymers and branched clusters (1.22−1.53).[40,41] The aggregation number of C_{18}-PEtOx-OH micelles in a solution of concentration 1.0 g L^{-1}, estimated from the apparent molar mass of the polymeric micelles obtained from SLS data and the molecular weight of the polymer, was of the same order of magnitude as the N_{agg} values reported for semitelechelic PEO or PNIPAM (∼16−30, depending on the molecular weight of the polymer and the solution concentration).[42] In contrast, micelles of the C_{18}-PiPrOx-OH samples were significantly smaller (N_{agg} ∼ 7). To confirm this finding, we carried out a series of fluorescence quenching experiments. The method, designed originally by Turro and Yekta[43] to determine the aggregation number of surfactant micelles, can be applied also to micelles of amphiphilic polymers, as a qualitative measure of trends in aggregation numbers.[24,36] The quencher was cetylpyridinium chloride (CPC), pyrene was the fluorescence probe, and the polymer. The N_{agg} values of the polymeric micelles, over a concentration range of 2.0−6.0 g L^{-1}, derived from fluorescence quenching were of the same order of magnitude as the values obtained by SLS (Table 2).

We turn our attention next to aqueous solutions of the telechelic polymers. Micelles formed by C_{18}-PEtOx-C_{18} in water

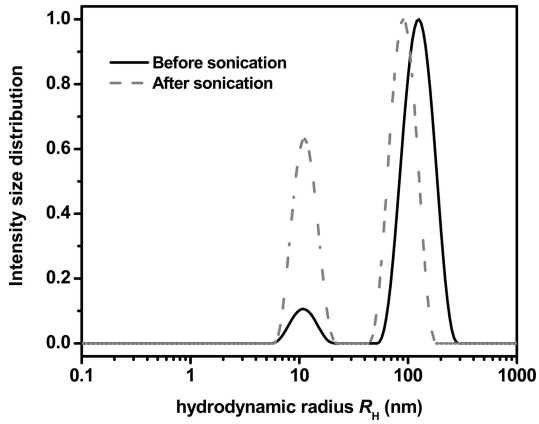

Figure 5. Effect of sonication (15 min) on the particles size distributions in an aqueous solution of C_{18}-PiPrOx-C_{18} 10K (polymer concentration: 1.0 g L^{-1}, temperature 24 °C, $\Theta = 90°$).

are smaller and more compact than the micelles formed by the corresponding semitelechelic polymer (Table 2). These data are consistent with a flowerlike micellar morphology, with no sign of intermicellar bridging in solutions within the 1.0−10.0 g L^{-1} concentration range tested here. The C_{18}-PiPrOx-C_{18} samples dissolved readily in water, but DLS analysis of the solutions revealed the coexistence of two populations of particles: small objects of $R_H \sim 8-10$ nm and larger objects of $R_H \sim 100-130$ nm. The fraction of large objects was predominant in solutions of C_{18}-PiPrOx-C_{18} 10K and C_{18}-PiPrOx-C_{18} 13K. Sonication of telechelic PiPrOx 10K solutions affected their composition, enhancing the fraction of small objects, as depicted in Figure 5, where we present the size distributions recorded for solutions of C_{18}-PiPrOx-C_{18} 10K before and after a 15 min sonication. Prolonged sonication did not bring about further changes in size distribution. For solutions of the shortest telechelic PiPrOx sample, however, sonication (15 min) led to a unimodal distribution of particles with $R_H \sim 7.6$ nm and $R_G/R_H = 1.20$, a value similar to the ratio recorded in the case of C_{18}-PEtOx-C_{18}. The larger objects observed in solutions of C_{18}-PiPrOx-C_{18} 10K and C_{18}-PiPrOx-C_{18} 13K may be clusters of several flower micelles linked to each other via bridging chains.

We determined the critical association concentrations of the polymers in water by fluorescence spectroscopy using pyrene (Py) as probe. In aqueous micellar solutions, Py, which is poorly soluble in water, is preferentially solubilized within hydrophobic microdomains. The ratio I_1/I_3 of the intensities of the first to third bands of the pyrene emission takes a value (∼1.8) for Py in water and decreases to ≅1.0−1.1, when Py is solubilized in nonpolar media, such as alkanes or within the hydrophobic core of surfactant micelles.[44] Thus, the amphiphile concentration for which a decrease in I_1/I_3 value occurs gives an estimate of the amphiphile critical micellar concentration. Plots of the changes in the ratio I_1/I_3 as a function of polymer concentration are presented in Figure 6 for solutions C_{18}-PiPrOx-OH (Figure 6, top) and C_{18}-PiPrOx-C_{18} (Figure 6, bottom). The ratio remained constant (1.8) with increasing polymer concentration up to a point beyond which it decreased gradually toward a plateau value of ∼1.0 in the most concentrated solutions tested (3.0 g L^{-1}). The decrease took place over a very large concentration range, a feature characteristic of telechelic polymers which, unlike low molecular weight surfactants, do not assemble cooperatively.[37,45] We used the polymer concentrations corresponding to the onset of the drop of I_1/I_3, indicated by arrows in Figure 6, as an estimate of the lowest polymer concentration, c_{mic}, for which hydrophobic domains able to host Py molecules form in solution via assembly of the end groups (Table 2). For the three PiPrOx pairs, the c_{mic} of the telechelic polymer was

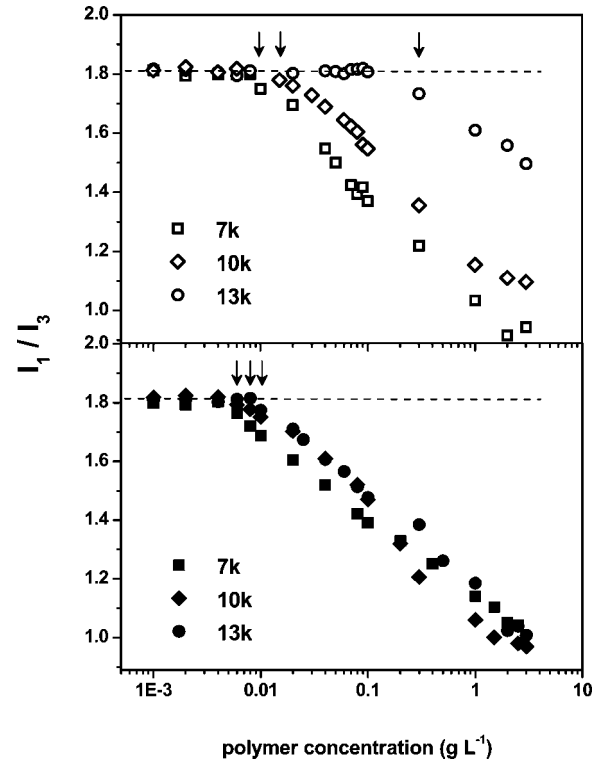

Figure 6. Changes in the ratio I_1/I_3 of the intensity of the first and third vibronic bands of pyrene (10^{-6} M) as a function of polymer concentration for solutions of C_{18}-PiPrOx-OH (open symbols) and C_{18}-PiPrOx-C_{18} (closed symbols) samples at 24 °C. The arrows indicate the concentration corresponding to the c_{mic} of each polymer (see text).

lower than that of the semitelechelic sample of identical molar mass. It increased with increasing polymer molecular weight for the semitelechelic samples. A similar trend was reported previously in a study of α-*n*-octadecyl-ω-hydroxypoly(2-methyl-2-oxazolines), with c_{mic} values ranging from 0.007 g L^{-1} ($M_n \sim 3200$ g mol^{-1}) to 0.05 g L^{-1} ($M_n \sim 8500$ g mol^{-1}).[24] For polymers of similar molecular weights, $M_n \sim 7000$ and 8500 g mol^{-1}, respectively; the c_{mic} of C_{18}-PiPrOx-OH is ∼5 times lower than that of C_{18}-PMeOx-OH, indicating the enhanced hydrophobicity of the PiPrOx chain compared to PMeOx. For pyrene solutions of C_{18}-PiPrOx-OH 13K, the I_1/I_3 value did not decrease below 1.5 even at the highest polymer concentration probed, implying that the probe environment remains hydrophilic in these solutions. This observation confirms the reluctance of C_{18}-PiPrOx-OH 13K to micellize in water, as noted above on the basis of LS data.

A series of SAXS measurements were performed to get information on the relative sizes of the core and the shell of the micelles. Scattering curves for solutions of telechelic /semitelechelic PEtOx 10K and PiPrOx 10K are presented in Figure 7 (top and bottom, respectively). The shapes of the curves recorded for solutions of concentration 2.0 and 20.0 g L^{-1} are similar, allowing us to assume that models based on noninteracting spheres are valid for interpretation of data gathered with solutions of 20.0 g L^{-1} polymer. Qualitatively, one notes that in the high q region the curves recorded for C_{18}-PAkOx-C_{18} are more structured than those obtained for the corresponding semitelechelic polymer, indicating that the electron density transition between micelles and water is sharper in solutions of the telechelic samples, compared to their semitelechelic counterparts. The experimental scattering curves were fitted according to three models: (i) polydisperse spheres, (ii) polydisperse spheres of core−shell structure with constant shell density, and (iii) polydisperse spheres of core−shell structure with a shell

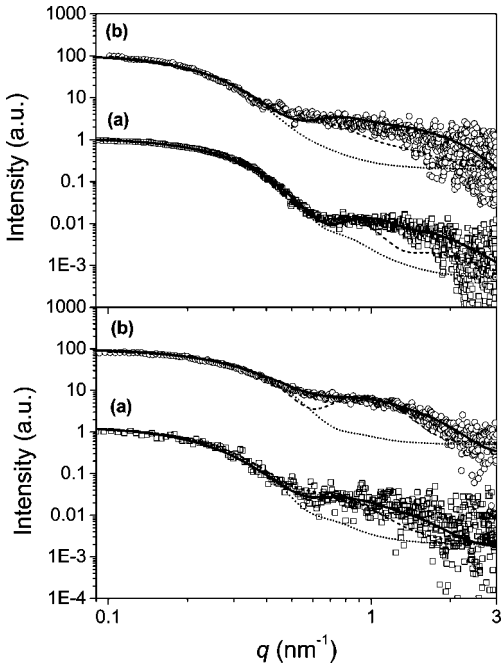

Figure 7. Experimental SAXS intensities for micellar solutions of telechelic (squares (a)) and semitelechelic (circles (b)) HM-PEtOx 10K (top) and HM-PiPrOx 10K (bottom). Lines are for comparison of fit curves from models of increasing complexity: (i) polydisperse spheres (dotted lines), (ii) polydisperse spheres of core−shell structure with constant shell density (dashed lines), and (iii) polydisperse sphere of core−shell structure with a shell density profile proportional to $r^{-\alpha}$ (solid lines). Polymer concentration: 20.0 g L^{-1}, temperature 24 °C. Note that curves (b) have been multiplied by a factor of 100 for clarity of presentation.

density profile proportional to $r^{-\alpha}$, where r is the distance from the core to the outer layer of the micelle and α is a scaling parameter which depends on the quality of the solvent. Best fits to the experimental curves were obtained by using the third model (see Figure 7). The core radius (R_{core}), the overall radius of the micelles ($R_{micelle}$), the ratio, ρ, of the shell to the core electron densities, and the radius of gyration (R_G^{SAXS}) are listed in Table 3. The radius of the micellar core ranged from 1.2 to 1.4 nm, which is on the order of magnitude of the length of an *n*-octadecyl chain in the all-trans configuration [~2.3 nm: 17 × 0.1265 nm (methylene groups) + 0.15 nm (terminal methyl group)]. The number of alkyl chains per core was calculated by dividing the volume of the core ($4/3\pi R_c^3$) by the volume of an octadecyl chain (0.311 nm^3). This results in a number of about 23 (R_c = 1.2 nm) to 37 (R_c = 1.4 nm) octadecyl chains or 11 to 18 polymer chains per micelle. By comparing the characteristics of the micelles formed by PiPrOx and PEtOx chains (M_n 10 000 g mol^{-1}), one notes that the core is smaller in the case of the PEtOx samples while the overall size of the micelle is larger. These features, together with the higher electron density contrast between the shell and the core in the case of the PEtOx micelles, may indicate that the corona of PEtOx micelles is more hydrated then the PiPrOx micellar corona. Within the series of telechelic PiPrOx, the core size increases slightly with increasing polymer molecular weight. In all cases, we observe higher SAXS intensities at low q values for micelles of the telechelic polymers, compared to the semitelechelic polymers micelles. Taking into account that the radii of the micelles are similar, it must be concluded that the density difference between shell and water is considerably higher for the micelles of the telechelic polymers than for the semitelechelic. This strongly argues in favor of the presence of flower micelles. Furthermore, the scattering intensity bends slightly downward in the low q region for micelles of C_{18}-PEtOx-OH 10K and C_{18}-PiPrOx-OH 10K. This hints toward repulsive interactions between the micelles of the semitelechelic polymers. Hence, the coronae of the semitelechelic micelles penetrate mutually, while the telechelic polymer micelles, in comparison, act more like hard spheres.

Comparing data extracted from SAXS and LS measurements, we note that the R_G values of the micelles obtained by LS are larger than those obtained by SAXS. Several factors may lead to this discrepancy. There are intrinsic differences between the two techniques: the R_G value derived from SAXS measurements is based on the differences in electron density between the micelles and their environment, while LS-derived values reflect differences in refractive index between micelles and their surroundings. Also, the measurable wavenumber by LS is smaller than by SAXS. Thus, if the LS data contain a contribution from large micellar aggregates, which are not detected by SAXS, size estimated via LS become larger than single micelles. Moreover, LS measurements were carried out with solutions of concentration 1.0 g L^{-1}, while SAXS data were acquired with more concentrated solutions (2.0−30 g L^{-1}) for which intermicellar interactions may influence the size of individual micelles.

Temperature Dependence of the Self-Assembly of Modified Poly(2-alkyl-2-oxazolines) in Water. Turbidity measurements confirmed that aqueous solutions of all semitelechelic and telechelic PAkOx described here undergo a heat-induced phase transition. The cloud points of the various polymers (solution concentration: 1.0 g L^{-1}) are listed in Table 1. A detailed thermodynamic analysis of the solution phase transition will be reported elsewhere.[46] In the following sections, we focus on the heat-induced changes in polymer self-assembly detected by ^{1}H NMR spectroscopy, LS, and fluorescence depolarization measurements. Figure 8 presents ^{1}H NMR spectra of C_{18}-PiPrOx-C_{18} 13K in D_2O at various temperatures. At 25 °C, the PAkOx chains are fully hydrated and flexible, giving rise to well-resolved and sharp resonances. Signals due to resonances of the *n*-octadecyl methylene protons (δ = 1.24 ppm, Figure 8, left) are weak and poorly resolved as a consequence of the confinement of the alkyl chains in the core of the micelles. As the C_{18}-PiPrOx-C_{18} 13K solution was heated beyond its cloud point (~35 °C in D_2O), the intensity of the PiPrOx protons resonances, such as the signal at δ = 1.06 ppm due to the isopropyl methyl groups, decreased gradually. The signals almost disappeared in spectra of solutions of T > 45 °C, indicating a decrease in the mobility of the dehydrated PiPrOx chain. Similar phenomena have been described in great detail for aqueous solutions of PNIPAM.[47] Note, however (Figure 8, right), that the decline in signal intensity is initiated only when the solution reaches a temperature *higher than* T_{cp} (e.g., $T = T_{cp}$ + 2 °C). For typical heat-sensitive polymer solutions, such as PNIPAM in D_2O, the main-chain protons signals decrease in intensity for temperature slightly *below* T_{cp} and vanish as the solution temperature barely exceeds T_{cp}.[47] Our results imply that the polymer chains still possess significant mobility in aqueous solutions beyond their cloud point.

Temperature-dependent light scattering measurements were carried out following a procedure (see Experimental Section) designed to achieve equilibrium conditions before each measurement and to avoid PiPrOx crystallization known to occur upon prolonged heating.[22] For all solutions, the size of the micelles remained constant upon heating from 25 °C to ~ T_{cp}. For $T > T_{cp}$, association of the micelles took place, as illustrated in Figure 9. Focusing first on solutions of the semitelechelic polymers C_{18}-PiPrOx-OH 10K (top) and C_{18}-PiPrOx-OH 7K (top), we note that the size of the aggregates increases sharply, reaching an R_H value of ~ 400 and 700 nm, respectively, for $T = T_{cp}$ + 4 °C. This increase in size is concomitant with a

Table 3. Characteristics of the Micelles of Various HM-PAkOx Samples in Aqueous Solutions (20 °C)[a]

polymer	c/g L^{-1}	R_{core}/nm	$R_{micelle}$/nm	ρ	σ	α	R_G^{SAXS}/nm[b]
C_{18}-PEtOx-OH 10K	20	1.2	11.7	0.002	0.15	1.33	7.5
C_{18}-PiPrOx-OH 7K	10	1.3	9.5	0.0027	0.09	1	7.8
C_{18}-PiPrOx-OH 10K	20	1.4	11.2	0.0015	0.13	1.33	9.3
C_{18}-PiPrOx-OH 13K	30						4.2[c]
C_{18}-PEtOx-C_{18} 10K	20	1.2	9.2	0.006	0.15	1	9.7
C_{18}-PiPrOx-C_{18} 7K	10	1.3	8.9	0.0029	0.08	1.1	7.3
C_{18}-PiPrOx-C_{18} 10K	20	1.4	11.1	0.0036	0.16	1.1	9.1
C_{18}-PiPrOx-C_{18} 13K	20	1.4	8.6	0.006	0.2	1.2	7.1

[a] Represented fit parameters are: R_{core}: radius of the core; $R_{micelle}$: overall radius of the core/shell spheres; ρ: ratio of shell/core electron densities; σ: relative standard deviation of particle radius; α: scaling parameter. [b] Calculated according to Föster and Burger (ref 31). [c] Radius of gyration for a Gaussian coil from Debye fit. Polymer concentration: 10−30 g L^{-1}.

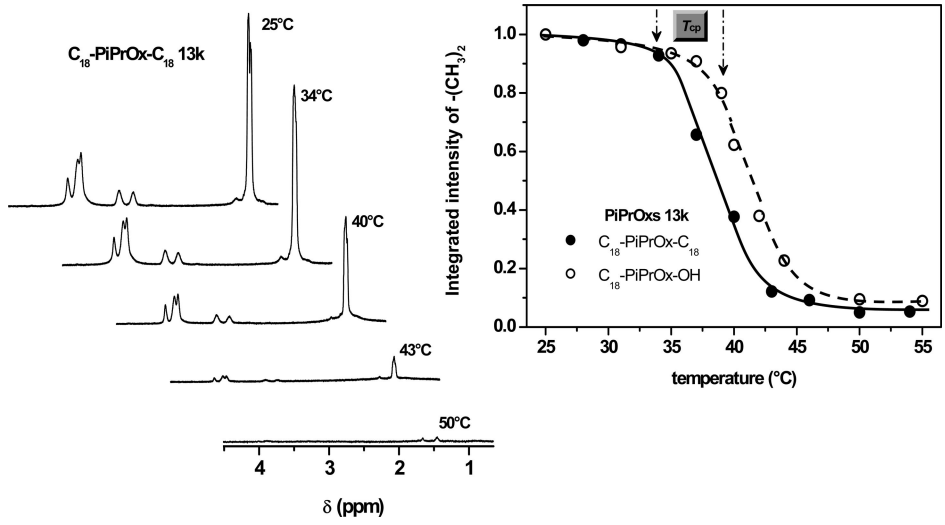

Figure 8. (left) Temperature-dependent ^{1}H NMR spectra of a solution of C_{18}-PiPrOx-C_{18} 13K in D_2O. (right) Changes as a function of temperature of the signal at 1.06 ppm assigned to the side-chain methyl protons of telechelic and semitelechelic PiPrOx 13K. The data are normalized to the intensity recorded at 25 °C. Polymer concentration: 2.0 g L^{-1}.

sharpening of the particle size distribution (PDI $\sim 0.02 \pm 0.01$). Further increase in temperature induces a decrease in R_H, which reaches a plateau value of ~260 nm (PDI $\sim 0.04 \pm 0.01$) once the solution temperature exceeds 45 °C. When solutions of telechelic PiPrOx were heated beyond their cloud points, extensive intermicellar association occurred leading to micron-sized aggregates. Their size was estimated from measurements carried out using a Nano ZS (Malvern) instrument designed to minimize the interference from multiple scattering (see Experimental Section). The R_H of the aggregates formed in a solution (1.0 g L^{-1}) of C_{18}-PiPrOx-C_{18} 13K heated at 35 °C was 1.3 μm (see Figure S1.3, Supporting Information). Further heating of the solutions triggered a shrinking of the aggregates, which ranged in R_H values from ~ 370 nm for the shortest polymer to ~ 715 nm for the longest (Figure 9, bottom). For these samples DLS measurements were performed at different scattering angles (40°−150°). Plots of ln $[G_1(t)]$ vs q^2t appear to be straight lines with a small upward deviation from the straight line for 150° (see Figure SI.2.1-2). This deviation is an indication of a significant polydispersity of the aggregate size. One can envisage two mechanisms whereby the associates drop in size after having reached a maximum value for T_{cp}: (i) particles split into smaller objects due to solution fluctuations occurring as the chains dehydrate, or (ii) each particle shrinks as a result of dehydration, much like thermosensitive gels for which the hydrophobic cores act as cross-linking agents. When solutions of the semitelechelic polymer C_{18}-PiPrOx-OH 13K, which does not micellize in cold water, were brought above their T_{cp}, large aggregates ($R_H \sim$ 880 nm) formed over a narrow temperature domain. Their size did not increase upon further heating. This behavior, which is typical of unmodified PiPrOx, leads us to conclude that the post-T_{cp} shrinking exhibited by the other polymers is a consequence of their association into micelles in cold solutions.

We carried out temperature-dependent fluorescence depolarization studies on polymer solutions doped with low amounts of the hydrophobic probe diphenylhexatriene (DPH). This probe is known to solubilize preferentially in hydrophobic alkylated environments, such as lipid bilayers. Typical anisotropy values for DPH in lipid bilayers[48] or in hydrophobically modified water-soluble polymers range from 0.20 to 0.30.[49] We measured first the temperature-induced changes in fluorescence anisotropy of DPH in a solution of the unmodified polymer (Me-PiPrOx-OH 10K). The anisotropy recorded for the cold solution was very small (~ 0.04), as expected since this polymer does not associate in cold water, providing no hydrophobic microdomains to accommodate the probe which remains dissolved in water. As the Me-PiPrOx-OH solution reached T_{cp}, the anisotropy reached a value in the vicinity of the limiting anisotropy ($r_0 \sim 0.362 \pm 0.015$) of DPH[48] (Figure 10). This large anisotropy enhancement indicates that the probe, solubilized within the polymer-rich phase that separates above the solution LCST, senses a rigid environment. Next, we determined the fluorescence anisotropy of DPH in cold solutions of C_{18}-PiPrOx-OH 10K and C_{18}-PiPrOx-C_{18} 10K (1.0 g L^{-1}, 17 °C) and of C_{18}-PEtOx-OH 10K and C_{18}-PEtOx-C_{18} 10K. It took values between ~ 0.22 and ~ 0.27 (Figure 10), confirming that DPH is solubilized preferentially in the alkyl-rich core of the polymer micelles. The anisotropies recorded for solutions of hydrophobically modified (HM) PiPrOx were somewhat larger than the values measured for HM-PEtOx solutions, implying that the core of HM-PiPrOx micelles is more compact than the core of HM-PEtOx micelles, in agreement with conclusions drawn from

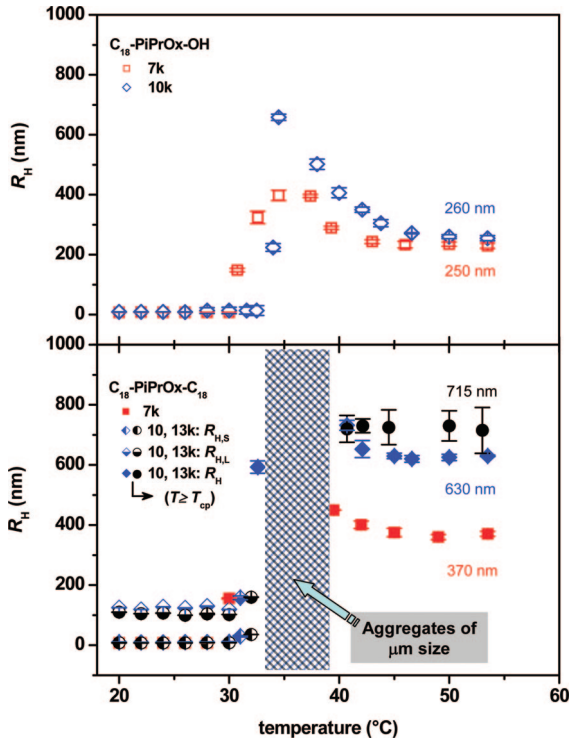

Figure 9. Changes with temperature of the hydrodynamic radii recorded by DLS analysis of aqueous solutions of C_{18}-PiPrOx-OH (top) and C_{18}-PiPrOx-C_{18} (bottom). The half-filled symbols (diamonds and circles, lower panel) represent the hydrodynamic radii of small ($R_{H,S}$) and large ($R_{H,L}$) objects in the case of bimodal size distributions (see text). The shaded area represents the temperature range in which the size of the aggregates cannot be measured under conditions used to collect the other data points (see text).

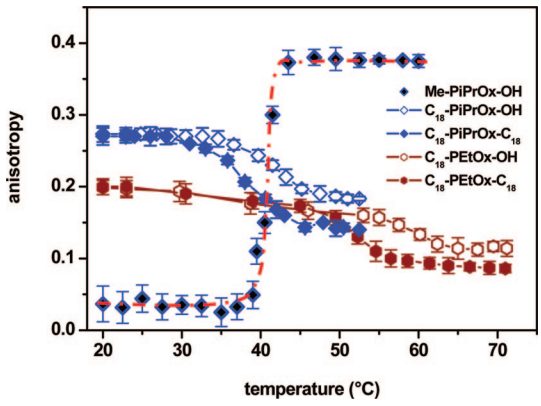

Figure 10. Changes in fluorescence anisotropy of DPH as a function of temperature for aqueous solutions of Me-PiPrOx-OH 10K, HM-PiPrOx 10K, and HM-PEtOx 10K (polymer concentration: 1.0 g L^{-1}).

SAXS data (see above). Upon heating solutions of HM-PiPrOx and HM-PEtOx beyond their respective cloud point, the fluorescence anisotropy *decreased slightly* (to approximately 0.20 and 0.12, respectively), an indication that the DPH environment becomes more fluid as a consequence of the heat-induced phase transition. The difference in the DPH anisotropy in Me-PiPrOx-OH aggregates ($\sim 0.38 \pm 0.02$) and in HM-PiPrOx aggregates ($\sim 0.28 \pm 0.01$) implies either that the alkyl core of the polymer micelles is mostly preserved within the particles formed above the solution cloud point or that the octadecyl chain ends, acting as "plasticizers", foil the rigid assembly of the dehydrated PiPrOx chains. Temperature-dependent SAXS experiments are in progress in order to determine the inner structure of the aggregates.

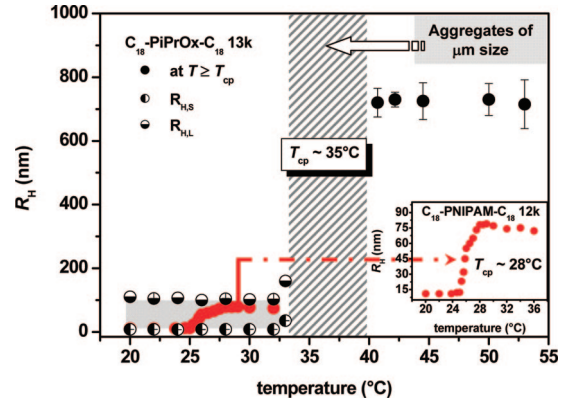

Figure 11. Temperature dependence of the hydrodynamic radii of C_{18}-PiPrOx-C_{18} 13K and C_{18}-PNIPAM-C_{18} 12K micelles. Polymer concentration: 1.0 g L^{-1}. The shaded area represents the temperature range in which the size of the aggregates cannot be measured under conditions used to collect the other data points (see text).

Conclusion

The analysis of aqueous solutions of telechelic and semi-telechelic HM-PiPrOx and HM-PEtOx by SLS, DLS, SAXS, ^{1}H NMR spectroscopy, and fluorescence spectroscopy led to the following description of the polymer self-assembly in water. In cold dilute aqueous solution, the polymers form micelles which may exist either as isolated entities or as clusters, depending on the solution concentration and the length of the polymer main chain. As the solutions are heated through and beyond their cloud point, the micelles or clusters of micelles form larger objects in which the PAkOx main chains retain their flexibility, until the solution exceeds a temperature well beyond T_{cp}. Eventually, when the temperature exceeds approximately $T_{cp} + 2$ °C, rigid objects form and their size remains constant upon further heating. These general features are reminiscent of the behavior of aqueous telechelic C_{18}-PNIPAM-C_{18} solution, as we anticipated since the monomer units of PNIPAM and PiPrOx are structural isomers. However, a closer examination of data gathered for the two families of HM polymers unveiled striking differences which reveal the impact of the main chain motif on the self-assembly of the two isomeric polymers. To illustrate this point, we plot in Figure 11 the temperature dependence of the hydrodynamic radii of C_{18}-PiPrOx-C_{18} 13K and C_{18}-PNIPAM-C_{18} 12K micelles (1.0 g L^{-1}). The C_{18}-PNIPAM-C_{18} 12K sample forms flower micelles in cold water ($R_H \sim 11$ nm).[50] Upon heating above the cloud point (28 °C), individual micelles associate into larger objects ($R_H \sim 75$ nm) as the solution temperature reaches 31 °C, the temperature corresponding to the coil-to-globule collapse of the PNIPAM chains.[7] Comparing these data with results reported here for telechelic PiPrOx, we note that (i) below the cloud point the micellar size distribution of C_{18}-PNIPAM-C_{18} is monomodal, whereas it is bimodal for C_{18}-PiPrOx-C_{18} 13K; (ii) for $T > 31$ °C, the C_{18}-PNIPAM-C_{18} micelles associate to form mesoglobules which have a R_H nearly 10 times smaller than the R_H of the C_{18}-PiPrOx-C_{18}13K assemblies formed under similar conditions; and (iii) the growth with temperature of the C_{18}-PNIPAM-C_{18} mesoglobules proceeds gradually toward the final size, without forming intermediate micron-sized aggregates, as in the case of C_{18}-PiPrOx-C_{18} 13K. In addition, the temperature-dependent fluorescence depolarization data suggest that the hydrophobic core of the C_{18}-PiPrOx-C_{18} 13K micelles is preserved within the aggregates formed in solutions at $T > T_{cp}$, whereas for C_{18}-PNIPAM-C_{18} samples, the micellar core disintegrates within the mesoglobules, as shown via temperature-dependent small-angle neutron scattering measurements.[51]

Unlike PNIPAM, PiPrOx is held in a rigid extended conformation by the main-chain amide nitrogen. Under conditions of steric confinement, such as the corona of star/flower micelles, hydration of the PiPrOx chain is restricted, and water molecules may act as intercalates between two neighboring chains, as suggested by Naumann et al.[52] in their study of the rheological properties of Langmuir monolayers of poly(2-ethyl-2-oxazoline)- or poly(2-methyl-2-oxazoline)-based lipopolymers at the air/water interface. This interchain cross-linking via water molecules leads to a reduction of the conformational entropy of the PiPrOx chains, affects the heat-induced association of dehydrated micelles, and may account for the large size of the aggregates formed in solutions heated above T_{cp}. The phenomenological study reported here constitutes merely the first step toward the establishment of the mechanism of hydration/dehydration of the PiPrOx chain in core−shell micelle. Further work is in progress aimed at assessing by calorimetry the thermodynamic parameters associated with the phase transition.

Acknowledgment. We thank Dr. P. Kujawa for critical reading of the manuscript and for valuable comments and Dr. X. X. Zhu (University of Montreal) for use of a Nanosizer Nano ZS light scattering instrument. This work was supported by a research grant of the Natural Sciences and Engineering Research Council of Canada to F.M.W.

Supporting Information Available: Data analysis and representative plots for the determination of R_G, M_w, and the angular dependence of R_H by light scattering. This material is available free of charge via the Internet at http://pubs.acs.org.

References and Notes

(1) *Associative Polymers in Aqueous Solution*; Glass, J. E., Ed.; American Chemical Society: Washington, DC, 2000; Vol. *765*.
(2) Kaczmarski, J. P.; Glass, J. E. *Macromolecules* **1993**, *26* (19), 5149–5156.
(3) Xu, R.; Winnik, M. A.; Riess, G.; Chu, B.; Croucher, M. D. *Macromolecules* **1992**, *25* (2), 644–652.
(4) Poppe, A.; Willner, L.; Allgaier, J.; Stellbrink, J.; Richter, D. *Macromolecules* **1997**, *30* (24), 7462–7471.
(5) Desponds, A.; Freitag, R. *Langmuir* **2003**, *19* (15), 6261–6270.
(6) Khoukh, S.; Oda, R.; Labrot, T.; Perrin, P.; Tribet, C. *Langmuir* **2007**, *23* (1), 94–104.
(7) Schild, H. G. *Prog. Polym. Sci.* **1992**, *17* (2), 163–249.
(8) Gao, J.; Haidar, G.; Lu, X.; Hu, Z. *Macromolecules* **2001**, *34* (7), 2242–2247.
(9) Chen, F. P.; Ames, A. E.; Taylor, L. D. *Macromolecules* **1990**, *23* (21), 4688–4695.
(10) Van Durme, K.; Van Mele, B.; Bernaerts, K. V.; Verdonck, B.; Du Prez, F. E. *J. Polym. Sci., Part B: Polym. Phys.* **2005**, *44* (2), 461–469.
(11) Hua, F.; Jiang, X.; Li, D.; Zhao, B. *J. Polym. Sci., Part A: Polym. Chem.* **2006**, *44* (8), 2454–2467.
(12) Kujawa, P.; Watanabe, H.; Tanaka, F.; Winnik, F. M. *Eur. Phys. J. E* **2005**, *17* (2), 129–137.
(13) Kujawa, P.; Segui, F.; Shaban, S.; Diab, C.; Okada, Y.; Tanaka, F.; Winnik, F. M. *Macromolecules* **2006**, *39* (1), 341–348.
(14) Kujawa, P.; Tanaka, F.; Winnik, F. M. *Macromolecules* **2006**, *39* (8), 3048–3055.
(15) Woodle, M. C.; Engbers, C. M.; Zalipsky, S. *Bioconjugate Chem.* **1994**, *5* (6), 493–496.
(16) Waschinski, C. J.; Herdes, V.; Schueler, F.; Tiller, J. C. *Macromol. Biosci.* **2004**, *5* (2), 149–156.
(17) Adams, N.; Schubert, U. S. *Adv. Drug Delivery Rev.* **2007**, *59* (15), 1504–1520.
(18) Yang, Y.; Kataoka, K.; Winnik, F. M. *Macromolecules* **2005**, *38* (6), 2043–2046.
(19) Christova, D.; Velichkova, R.; Loos, W.; Goethals, E. J.; Du Prez, F. E. *Polymer* **2003**, *44* (8), 2255–2261.
(20) Diab, C.; Akiyama, Y.; Kataoka, K.; Winnik, F. M. *Macromolecules* **2004**, *37* (7), 2556–2562.
(21) Meyer, M.; Antonietti, M.; Schlaad, H. *Soft Matter* **2007**, *3* (4), 430–431.
(22) Demirel, A. L.; Meyer, M.; Schlaad, H. *Angew. Chem., Int. Ed.* **2007**, *46* (45), 8622–8624.
(23) Litt, M.; Rahl, F.; Roldan, L. G. *J. Polym. Sci., Polym. Phys. Ed* **1969**, *7*, 463–473.
(24) Volet, G.; Chanthavong, V.; Wintgens, V.; Amiel, C. *Macromolecules* **2005**, *38* (12), 5190–5197.
(25) Weberskirch, R.; Preuschen, J.; Spiess, H. W.; Nuyken, O. *Macromol. Chem. Phys.* **2000**, *201* (10), 995–1007.
(26) Seeliger, W.; Aufderhaar, E.; Diepers, W.; Feinauer, R.; Nehring, R.; Thier, W.; Hellmann, H. *Angew. Chem., Int. Ed.* **1966**, *5* (10), 875–888.
(27) *Surfactant Solutions: New Methods of Investigation*; Zana, R., Ed.; Marcel Dekker: New York, 1987.
(28) Gourier, C.; Beaudoin, E.; Duval, M.; Sarazin, D.; Maitre, S.; François, J. *J. Colloid Interface Sci.* **2000**, *230* (1), 41–52.
(29) Chassenieux, C.; Nicolai, T.; Durand, D. *Macromolecules* **1997**, *30* (17), 4952–4958.
(30) Meng, X.-X.; Russel, W. B. *Macromolecules* **2005**, *38* (2), 593–600.
(31) Förster, S.; Burger, C. *Macromolecules* **1998**, *31* (3), 879–891.
(32) Ma, S. X.; Cooper, S. L. *Macromolecules* **2001**, *34* (10), 3294–3301.
(33) Wetzel, W. H.; Chen, M.; Glass, J. E. *Associative Thickeners—An Overview with an Emphasis on Synthetic Procedures*; Glass, J. E., Ed.; American Chemical Society: Washington, DC, 1996; Vol. *248*.
(34) The Analysis of Pharmaceutical Substances and Formulated Products by Vibrational Spectroscopy. In *Handbook of Vibrational Spectroscopy*; Chalmers, J. M., Griffits, P. P., Eds.; Wiley: London, UK, 2002; Vol. *5*.
(35) Vorobyova, O.; Yekta, A.; Winnik, M. A.; Lau, W. *Macromolecules* **1998**, *31* (25), 8998–9007.
(36) Elliott, P. T.; Xing, L.; Wetzel, W. H.; Glass, J. E. *Macromolecules* **2003**, *36* (22), 8449–8460.
(37) Alami, E.; Almgren, M.; Brown, W.; François, J. *Macromolecules* **1996**, *29* (6), 2229–2243.
(38) Nakayama, M.; Okano, T. *Biomacromolecules* **2005**, *6* (4), 2320–2327.
(39) Berne, B. J.; Pecora, R. *Dynamic Light Scattering with Applications to Chemistry, Biology, and Physics*; Wiley: New York, 2000.
(40) Burchard, W. In *Light Scattering Principles and Development*; Brown, W., Ed.; Clarendon Press: Oxford: 1996; p 439.
(41) Matuschek, D. W.; Blumen, A. *Macromolecules* **1989**, *22* (3), 1490–1491.
(42) Ameri, M.; Attwood, D.; Collett, J. H.; Booth, C. *J. Chem. Soc., Faraday. Trans.* **1997**, *93* (15), 2545–2551.
(43) Turro, N. J.; Yekta, A. *J. Am. Chem. Soc.* **1978**, *100* (18), 5951–5952.
(44) Kalyanasundaram, K.; Thomas, J. K. *J. Am. Chem. Soc.* **1977**, *99* (7), 2039–2044.
(45) Petit-Agnely, F.; Iliopoulos, I.; Zana, R. *Langmuir* **2000**, *16* (25), 9921–9927.
(46) Obeid, R.; Tanaka, F.; Winnik, F. M., manuscript in preparation.
(47) Zeng, F.; Tong, Z.; Feng, H. *Polymer* **1997**, *38* (22), 5539–5544.
(48) Shinitzky, M.; Barenholz, Y. *Biochim. Biophys. Acta* **1978**, *515* (4), 367–94.
(49) Ringsdorf, H.; Venzmer, J.; Winnik, F. M. *Macromolecules* **1991**, *24* (7), 1678–1686.
(50) Kujawa, P.; Obeid, R.; Qiu, X.-P.; Winnik, F. M. *Polym. Prepr. (Am. Chem. Soc.)* **2006**, *47* (2), 794–795.
(51) Koga, T.; Tanaka, F.; Motokawa, R.; Koizumi, S.; Winnik, F. M. *Macromolecules* **2008**, *41* (23), 9413–9422.
(52) Naumann, C. A.; Brooks, C. F.; Fuller, G. G.; Lehmann, T.; Ruehe, J.; Knoll, W.; Kuhn, P.; Nuyken, O.; Frank, C. W. *Langmuir* **2001**, *17* (9), 2801–2806.

MA802592F